Article

Gold Nanoparticles on Mesoporous SiO$_2$-Coated Magnetic Fe$_3$O$_4$ Spheres: A Magnetically Separatable Catalyst with Good Thermal Stability

Huan Liu [1,†], **Chao Lin** [2,†], **Zhen Ma** [3,*], **Hongbo Yu** [4,*] **and Shenghu Zhou** [4]

[1] Research Institute of Applied Catalysis, Shanghai Institute of Technology, Shanghai 201418, China
[2] Department of Physics, Faculty of Science, Ningbo University, Ningbo 315211, China
[3] Shanghai Key Laboratory of Atmospheric Particle Pollution and Prevention (LAP^3),
    Department of Environmental Science and Engineering, Fudan University, Shanghai 200433, China
[4] Ningbo Institute of Materials Engineering and Technology, Chinese Academy of Sciences,
    Ningbo 315201, China

[†] These authors contributed equally to this work.

* Authors to whom correspondence should be addressed; E-Mails: zhenma@fudan.edu.cn (Z.M.);
    yuhongbo@nimte.ac.cn (H.Y.); Tel.: +86-574-8669-6927 (H.Y.); Fax: +86-574-8668-5043 (H.Y.).

Abstract: Fe$_3$O$_4$ spheres with an average size of 273 nm were prepared in the presence of CTAB by a solvothermal method. The spheres were modified by a thin layer of SiO$_2$, and then coated by mesoporous SiO$_2$ (m-SiO$_2$) films, by using TEOS as a precursor and CTAB as a soft template. The resulting m-SiO$_2$/Fe$_3$O$_4$ spheres, with an average particle size of 320 nm, a high surface area (656 m^2/g), and ordered nanopores (average pore size 2.5 nm), were loaded with gold nanoparticles (average size 3.3 nm). The presence of m-SiO$_2$ coating could stabilize gold nanoparticles against sintering at 500 °C. The material showed better performance than a conventional Au/SiO$_2$ catalyst in catalytic reduction of *p*-nitrophenol with NaBH$_4$. It can be separated from the reaction mixture by a magnet and be recycled without obvious loss of catalytic activity. Relevant characterization by XRD, TEM, N$_2$ adsorption-desorption, and magnetic measurements were conducted.

Keywords: solvothermal method; magnetic Fe$_3$O$_4$ spheres; *p*-nitrophenol; gold catalysis

1. Introduction

Gold was initially regarded as useless in catalysis, until Haruta and co-workers found that small gold nanoparticles supported on some reducible oxide supports can be highly active for CO oxidation [1–3]. This finding triggered a great deal of interest in exploring the application of gold catalysts in other reactions [4–6], such as organic catalysis [7–11]. Most of the heterogeneous gold catalysts reported so far involve oxide supports such as TiO_2, ZrO_2, Fe_2O_3, CeO_2, Al_2O_3, and SiO_2. These oxide supports are not magnetic, thus making the supported gold catalysts difficult to separate after conducting organic reactions. In addition, many gold catalysts tend to sinter under elevated temperatures due to the low melting points of gold nanoparticles. The sintering can occur even under mild reaction conditions in organic catalysis. Therefore, for the sake of practical applications, it is desirable to design magnetically separable gold catalysts with good thermal stability.

Fe_3O_4 is a magnetic oxide. It can be used for designing magnetically separable catalysts and other functional materials [12–20]. For instance, Yin and co-workers prepared $SiO_2/Au/Fe_3O_4$ catalysts by coating an Au/Fe_3O_4 catalyst with a SiO_2 matrix, followed by controlled etching [21]. That way, the gold nanoparticles were protected by the SiO_2 shell, and the SiO_2 shell was porous, allowing for the diffusion of reactants and products. Alternatively, Zhao and co-workers prepared $SiO_2/Au/Fe_3O_4$ catalysts by assembling a porous SiO_2 shell on top of an Au/Fe_3O_4 catalyst, with the aid of a soft template [22]. The resulting $SiO_2/Au/Fe_3O_4$ catalyst has enhanced stability against sintering. These $SiO_2/Au/Fe_3O_4$ catalysts are particularly useful in organic catalysis, because they can be separated from the liquid phase after reaction by simply using a magnet.

Here we prepare another catalyst, $Au/m\text{-}SiO_2/Fe_3O_4$ (Scheme 1). First, magnetic Fe_3O_4 particles were prepared by a solvothermal method. The particles were treated by a small amount of TEOS in the absence of a soft template (CTAB), and subsequently coated by mesoporous SiO_2 ($m\text{-}SiO_2$) films with the aid of the soft template. Gold nanoparticles were then deposited onto the $m\text{-}SiO_2$-coated Fe_3O_4 support. The resulting catalyst is magnetically separable, thermally stable, and shows better catalytic activity than Au/SiO_2 in the catalytic reduction of *p*-nitrophenol with $NaBH_4$.

Scheme 1. Synthesis of $Au/m\text{-}SiO_2/Fe_3O_4$ that can be separated by a magnet.
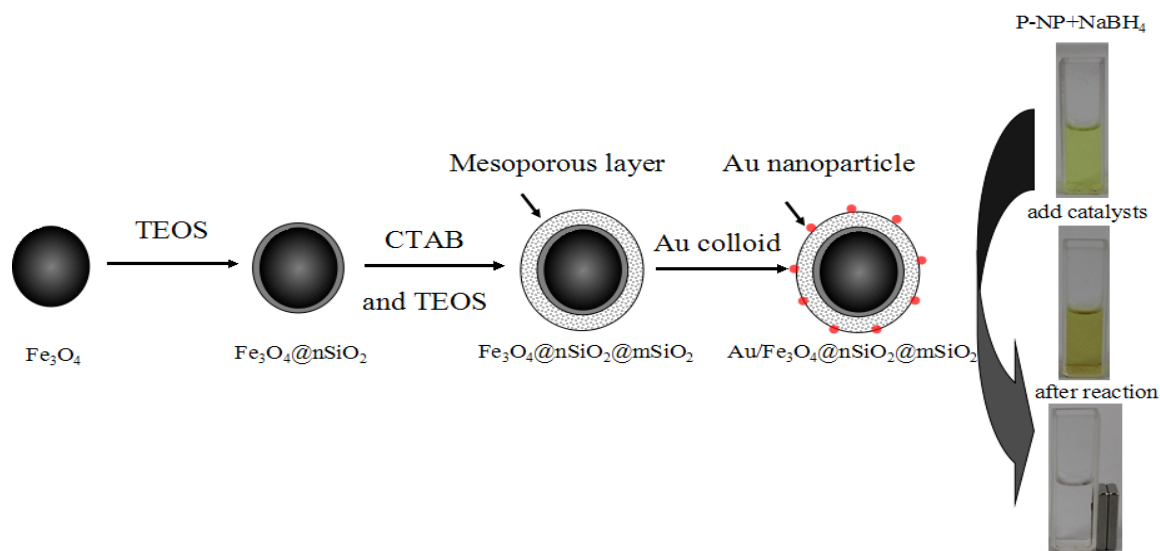
2. Results and Discussion

Many references have reported the synthesis of Fe_3O_4 spheres in the presence of a protecting agent [15,23–25]. The formation of Fe_3O_4 spheres generally involves nanocrystal nucleation, crystal growth, and self-assembly [24]. Our work used CTAB as a protecting agent. The synthesized Fe_3O_4 particles are spherical, as seen from the TEM and SEM images in Figure 1. The particle size distribution obtained from TEM analysis of a number of particles is shown in Figure S1 in the Supplementary Materials. The average particle size is 273 nm.

Figure 1. TEM (**a**) and SEM (**b**) images of Fe_3O_4 spheres.
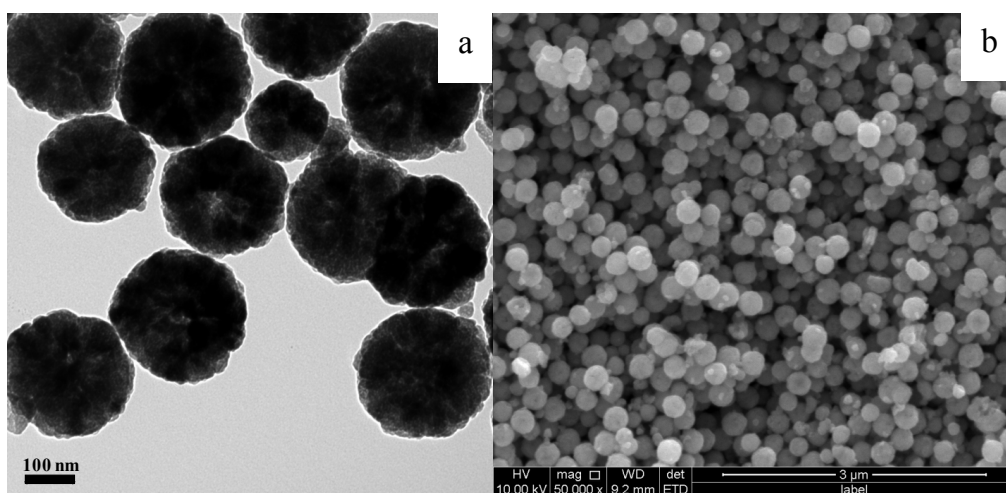

The Fe_3O_4 sample has characteristic XRD peaks at $2\theta = 30.2°$, 35.6°, 43.2°, 53.6°, 57.2°, 62.8°, and 74.2° (Figure 2a), corresponding to the cubic phase of Fe_3O_4.

Figure 2. XRD patterns of (**a**) Fe_3O_4 spheres; (**b**) m-SiO_2/Fe_3O_4 without calcination; (**c**) m-SiO_2/Fe_3O_4 calcined at 500 °C to remove the soft template; (**d**) Au/m-SiO_2/Fe_3O_4.
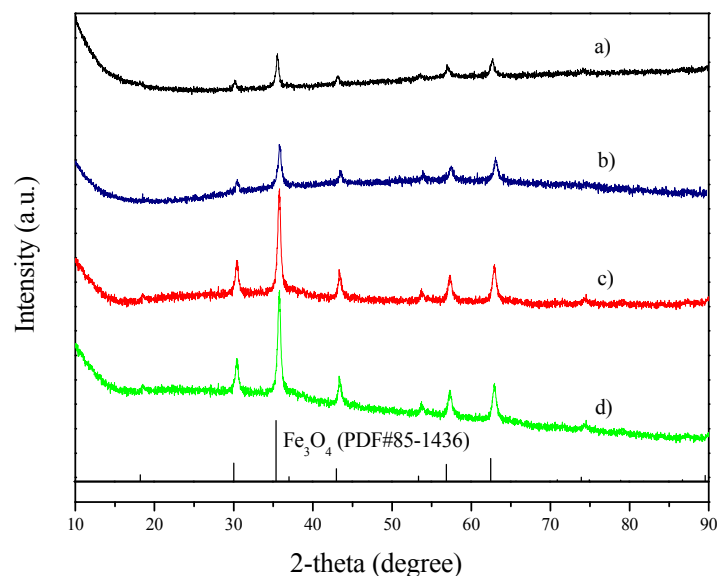
To synthesize m-SiO$_2$/Fe$_3$O$_4$, the Fe$_3$O$_4$ particles were first treated by a small amount of TEOS, resulting in the modification of Fe$_3$O$_4$ particles with a thin layer of SiO$_2$ (see Figure S2 in the Supplementary Materials). Then the SiO$_2$-modified Fe$_3$O$_4$ particles were treated with more TEOS in the presence of a soft template (CTAB), followed by calcination to remove the soft template, resulting in the formation of m-SiO$_2$/Fe$_3$O$_4$. The average size of m-SiO$_2$/Fe$_3$O$_4$ particles is about 320 nm, as seen from the TEM image in Figure 3. Figure 3 also shows that the thickness of the SiO$_2$ layer is about 27 nm, and the SiO$_2$ layer is porous. Figure S3 shows more TEM images of the sample.

Figure 3. TEM image of m-SiO$_2$/Fe$_3$O$_4$.
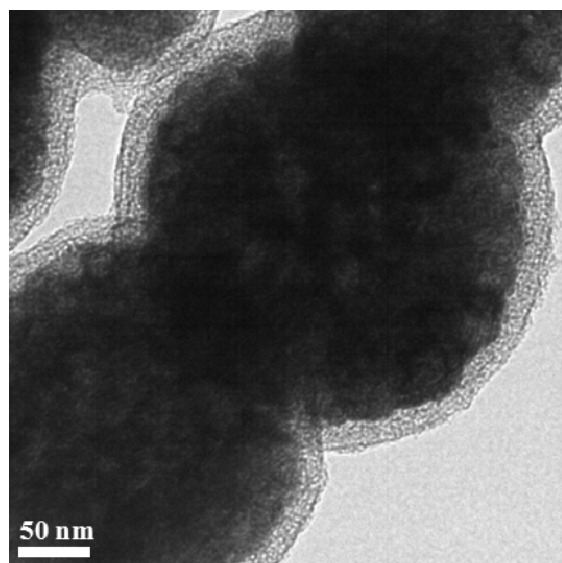
The material has a high surface area of 656 m^2/g and an average pore size of 2.5 nm (Figure 4). For comparison, the surface area of Fe$_3$O$_4$ particles is only 30 m^2/g.

Figure 4. The nitrogen adsorption-desorption isotherms and pore size distribution of m-SiO$_2$/Fe$_3$O$_4$.
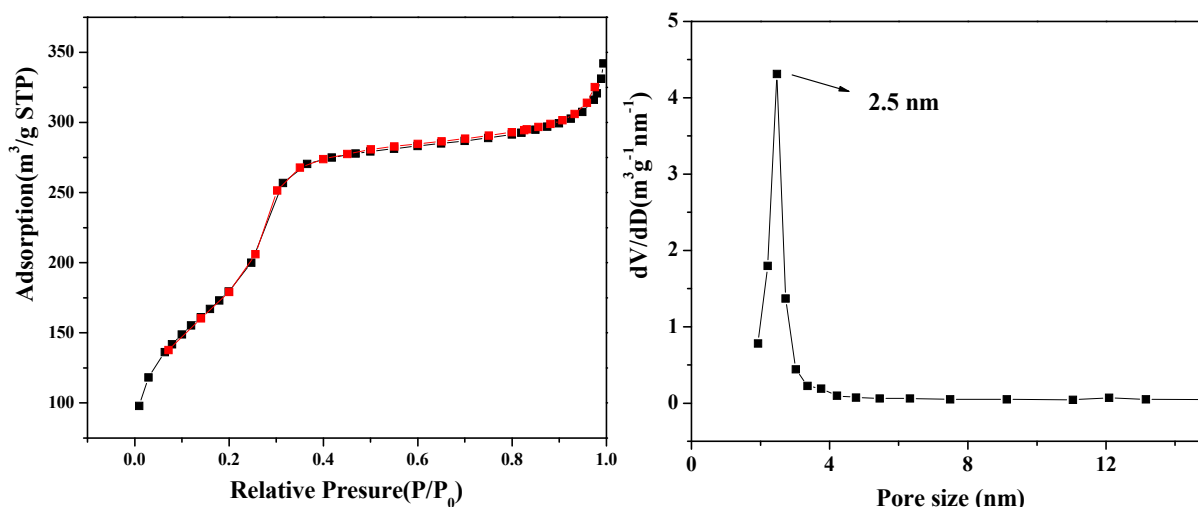
The SiO$_2$ coating is amorphous, as shown by the XRD data (Figure 2b,c). Note that the material was calcined at 500 °C to remove the soft template and create mesopores. This calcination process increases the crystallinity of the Fe$_3$O$_4$ particles, as seen from the sharper peaks in Figure 2c.

Figure 5 shows the magnetization curves of samples. The saturated susceptibility of Fe$_3$O$_4$ spheres is 65.0 emu/g. The modification of Fe$_3$O$_4$ spheres by a thin layer of SiO$_2$ leads to a negligible decrease in saturated susceptibility. The saturated susceptibility of m-SiO$_2$/Fe$_3$O$_4$ is 24.7 emu/g. The loading of gold nanoparticles onto m-SiO$_2$/Fe$_3$O$_4$ leads to a negligible decrease in saturated susceptibility.

Figure 5. Hysteresis loops of samples at room temperature: (**a**) Fe$_3$O$_4$ particles; (**b**) thin SiO$_2$-modified Fe$_3$O$_4$; (**c**) m-SiO$_2$/Fe$_3$O$_4$; (**d**) Au/m-SiO$_2$/Fe$_3$O$_4$.
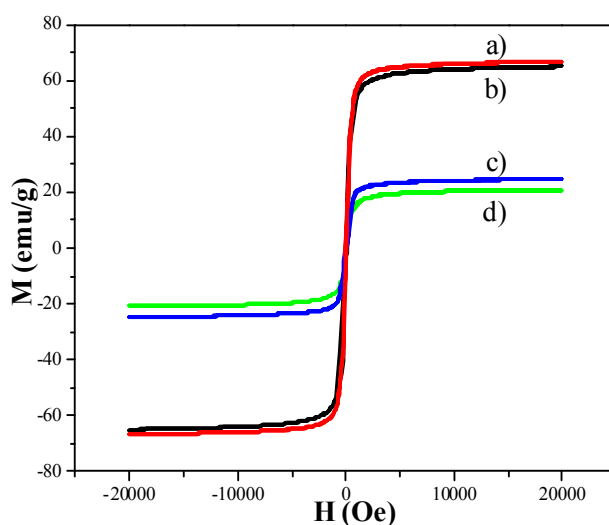
Thermal stability is an important factor for practical applications of gold catalysts. Figure 6 shows the TEM images of Au/m-SiO$_2$/Fe$_3$O$_4$ samples as prepared and calcined at 500 °C. For the as-prepared Au/m-SiO$_2$/Fe$_3$O$_4$, the gold nanoparticles are highly dispersed, with an average particle size of 3.3 nm. The particle size distribution is shown in Figure S4. When the Au/m-SiO$_2$/Fe$_3$O$_4$ is calcined at 500 °C for 2 h, the average gold particle size increases only slightly to 3.8 nm. On the other hand, the average size of gold nanoparticles in Au/SiO$_2$ increases from 3.4 nm to 13.4 nm after calcination at 500 °C. Although the average size of gold nanoparticles (3.3 nm) is larger than the average pore size of the mesoporous SiO$_2$ coating, the presence of mesoporous SiO$_2$ still mitigates the sintering of gold nanoparticles.

Catalytic reduction of *p*-nitrophenol by NaBH$_4$ was chosen to compare the performance of different gold catalysts. The reaction was carried out in a cuvette (rather than a round-bottom flask reported previously [26]) to allow for *in situ* monitoring. The reaction progress was followed by UV-Vis as the peak around 400 nm corresponds to the absorption of *p*-nitrophenol. Figure 7 shows the decreases in *p*-nitrophenol concentrations as the reaction proceeds. A faster decrease indicates higher catalytic activity. The conversions of *p*-nitrophenol on Au/m-SiO$_2$/Fe$_3$O$_4$ and Au/SiO$_2$ after 90 s reaction are 72.5% and 28.2%, respectively. After calcination at 500 °C, these catalysts show conversions of 49.4% and 4.5%, respectively. The catalysis data (also seen in Figure S5 and Table S1) again show the advantage of using a mesoporous SiO$_2$ coating. As the catalytic activity drops greatly when the size of gold nanoparticles is increased [26], the low activity of the sintered Au/SiO$_2$ catalyst is justified.

Figure 6. TEM images of as-synthesized Au/m-SiO$_2$/Fe$_3$O$_4$ (**a**), Au/m-SiO$_2$/Fe$_3$O$_4$ calcined at 500 °C (**b**), as-synthesized Au/SiO$_2$ (**c**) and Au/SiO$_2$ calcined at 500 °C (**d**).
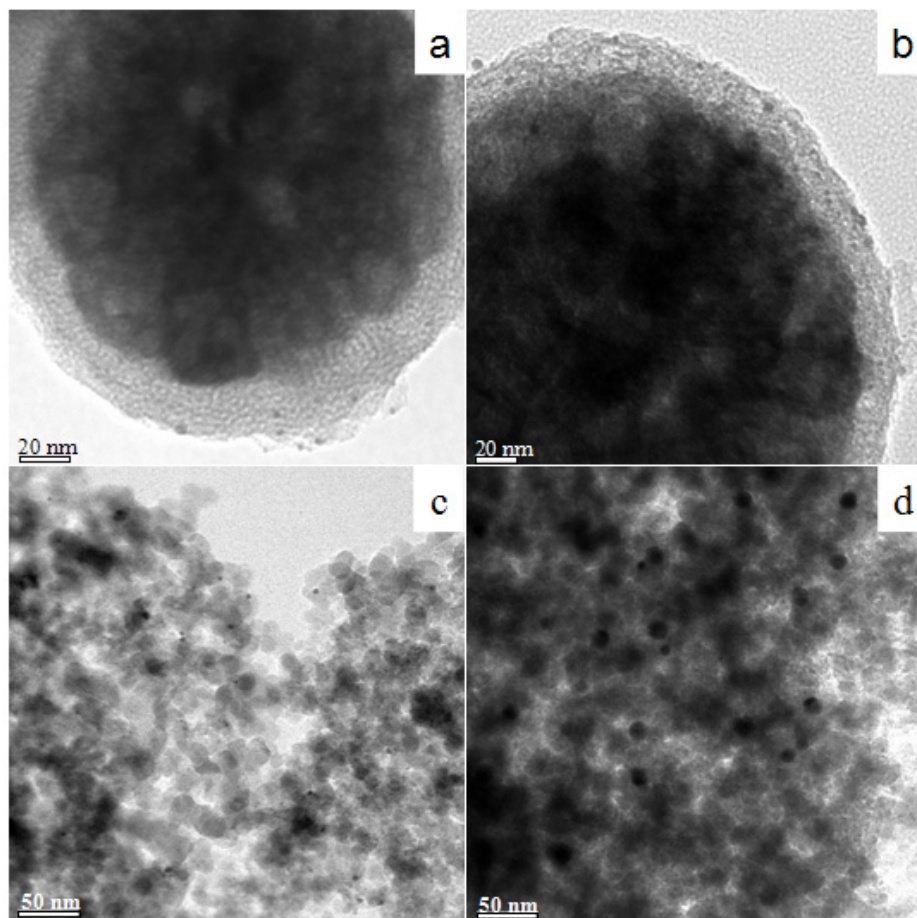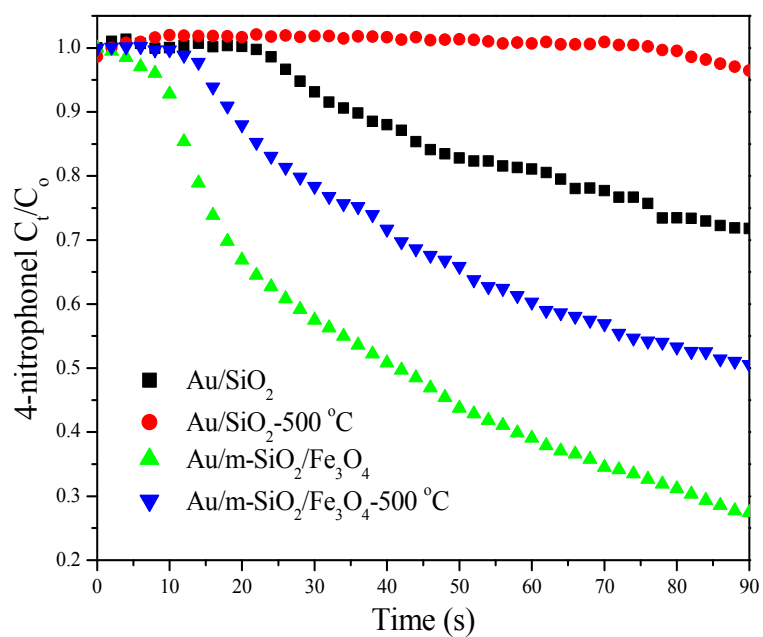

Figure 7. Decrease in *p*-nitrophenol's relative concentration during the hydrogenation reaction using different catalysts.

The catalyst recyclability was studied by testing the activity of Au/m-SiO$_2$/Fe$_3$O$_4$ after separation using a magnet (see the photos in Scheme 1). No additional catalyst was added into the liquid phase. As shown in Figure 8, Au/m-SiO$_2$/Fe$_3$O$_4$ shows stable activity in repeated runs.

Figure 8. Performance of Au/m-SiO$_2$/Fe$_3$O$_4$ in repeated runs, after recycling of the catalyst.
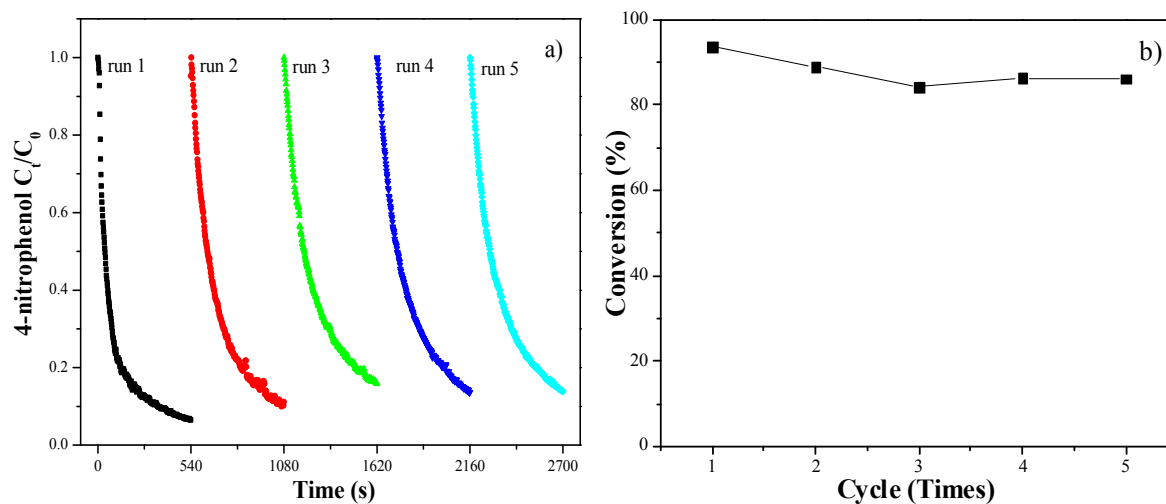
3. Experimental

3.1. Chemicals

All chemicals were used as received. Anhydrous FeCl$_3$, sodium acetate, ethylene glycol, aqueous ammonia, polyvinylprrolidone (PVP, MW-58000), *p*-nitrophenol was purchased from Sinopharm Chemical Reagent Co. (Shanghai, China). Tetraethoxysilane (TEOS), hexadecyl trimethyl ammonium bromide (CTAB), HAuCl$_4$·4H$_2$O and NaBH$_4$ were purchased from Aladdin Co. (Shanghai, China).

3.2. Catalyst Preparation

3.2.1. Preparation of Fe$_3$O$_4$ Spheres

Anhydrous FeCl$_3$ (0.54 g), CTAB (0.2 g) and sodium acetate (2.5 g) were dissolved in ethylene glycol (50 mL), transferred into an autoclave, and subjected to solvothermal treatment at 180 °C for 24 h. The obtained sample was washed by anhydrous ethanol and deionized water several times, and dried at room temperature.

3.2.2. Preparation of m-SiO$_2$/Fe$_3$O$_4$

Fe$_3$O$_4$ spheres (0.1 g) were dispersed in deionized water (100 mL), then aqueous ammonia (3 mL) and TEOS (0.3 mL) were added, and the mixture was stirred mechanically for 1 h. The solid was collected by a magnet, washed with deionized water and ethanol, and dried at room temperature.

The solid product mentioned above (0.1 g) was mixed with deionized water (100 mL). CTAB (0.2 g) aqueous ammonia (3 mL) was added, and the mixture was stirred at room temperature for 30 min. TEOS (2 mL) was then added, and the mixture was continuously stirred for 8 h. The obtained product

was washed with anhydrous ethanol and water several times, dried at 100 °C for 4 h, and calcined at 500 °C for 4 h. The resulting material is denoted as m-SiO_2/Fe_3O_4.

3.2.3. Preparation of Au/m-SiO_2/Fe_3O_4 and Au/SiO_2 Catalysts

To prepare gold colloids, $NaBH_4$ (19 mg) was dissolved in deionized water (5 g), and cooled in a refrigerator (5 °C). $HAuCl_4\cdot4H_2O$ (20 mg) and PVP (10 mg) were dissolved in deionized water (95 g). After stirring the mixture for 30 min, the $NaBH_4$ solution was injected. After stirring for 1 h, gold colloid solution (3 mL, containing 0.3 mg Au) were mixed with m-SiO_2/Fe_3O_4 spheres (0.1 g) or a conventional SiO_2 support (surface area 176 m^2/g), subjected to ultrasonic treatment for 10 min, and left standing for 10 min. The mixture was subjected to centrifugation after adding some water, and the obtained product was dried at room temperature. The theoretical gold content was 0.3 wt%, whereas the actual gold contents measure by ICP were 0.28 wt% and 0.30 wt%, respectively.

3.3. Characterization

XRD patterns were collected on a Bruker AXS D8 Advance diffractometer using Cu Kα radiation. SEM images were obtained by a FEI Quanta FEG 250 field-emission scanning electron microscope operated at 20 kV. TEM images were obtained by a Tecnai F20 transmission electron microscope operated at 200 kV. The surface areas were measured on an ASAP-2020 M analyzer. Magnetic properties were measured using MPMS SQUID VEM system. ICP analysis of gold content was conducted using Perkin-Elmer Optima 2100 instrument.

3.4. Catalytic Reduction of p-Nitrophenol with $NaBH_4$

Catalyst (10 mg) was dispersed in deionized water (50 mL) with the aid of ultrasonic treatment. 300 mM $NaBH_4$ solution (1 mL), 3 mM *p*-nitrophenol solution (0.05 mL), and water (1 mL) containing catalyst (mentioned above, 0.2 mg) was added into a cuvette, and the mixture was subjected to absorption measurement at 400 nm every 2 s, by using an UV-Vis-3300 spectrometer (Shanghai Meipuda, Shanghai, China).

4. Conclusions

An Au/m-SiO_2/Fe_3O_4 catalyst was prepared by using magnetic Fe_3O_4 spheres as a core and support, followed by coating the core with a porous SiO_2 shell via a "soft-templating" approach and deposition of gold nanoparticles. The catalyst showed higher activity than Au/SiO_2 in the catalytic reduction of *p*-nitrophenol with $NaBH_4$. It also showed good thermal stability. The mesoporous SiO_2 coatings play an important role in stabilizing supported gold nanoparticles.

Supplementary Materials

Supplementary materials can be accessed at: http://www.mdpi.com/1420-3049/18/11/14258/s1.

Acknowledgments

Conflicts of Interest

The authors declare no conflict of interest.

References

1. Haruta, M.; Kobayashi, T.; Sano, H.; Yamada, N. Novel gold catalysts for the oxidation of carbon-monoxide at a temperature far below 0 °C. *Chem. Lett.* **1987**, *16*, 405–408.
2. Haruta, M.; Yamada, N.; Kobayashi, T.; Iijima, S. Gold catalysts prepared by coprecipitation for low-temperature oxidation of hydrogen and of carbon monoxide. *J. Catal.* **1989**, *115*, 301–309.
3. Haruta, M.; Tsubota, S.; Kobayashi, T.; Kageyama, H.; Genet, M.J.; Delmon, B. Low-temperature oxidation of CO over gold supported on TiO_2, α-Fe_2O_3, and Co_3O_4. *J. Catal.* **1993**, *144*, 175–192.
4. Hashmi, A.S.K. The catalysis gold rush: New claims. *Angew. Chem. Int. Ed.* **2005**, *44*, 6990–6993.
5. Bond, G.C.; Louis, C.; Thompson, D.T. *Catalysis by Gold*; Imperial College Press: London, UK, 2006.
6. Takei, T.; Akita, K.; Nakamura, I.; Fujitani, T.; Okumura, M.; Okazaki, K.; Huang, J.H.; Ishida, T.; Haruta, M. Heterogeneous catalysis by gold. *Adv. Catal.* **2012**, *55*, 1–126.
7. Della Pina, C.; Falletta, E.; Prati, L.; Rossi, M. Selective oxidation using gold. *Chem. Soc. Rev.* **2008**, *37*, 2077–2095.
8. Corma, A.; Garcia, H. Supported gold nanoparticles for organic reactions. *Chem. Soc. Rev.* **2008**, *37*, 2096–2126.
9. Zhang, Y.; Cui, X.J.; Shi, F.; Deng, Y.Q. Nano-gold catalysis in fine chemical synthesis. *Chem. Rev.* **2012**, *112*, 2467–2505.
10. Stratakis, M.; Garcia, H. Catalysis by supported gold nanoparticles: Beyond aerobic oxidative processes. *Chem. Rev.* **2012**, *112*, 4469–4506.
11. Davis, S.E.; Ide, M.S.; Davis, R.J. Selective oxidation of alcohols and aldehydes over supported metal nanoparticles. *Green Chem.* **2013**, *15*, 17–45.
12. Deng, Y.H.; Qi, D.W.; Deng, C.H.; Zhang, X.M.; Zhao, D.Y. Superparamagnetic high-magnetization microspheres with an $Fe_3O_4@SiO_2$ core and perpendicularly aligned mesoporous SiO_2 shell for removal of microcystins. *J. Am. Chem. Soc.* **2007**, *130*, 28–29.
13. Xuan, S.H.; Jiang, W.Q.; Gong, X.L.; Hu, Y.; Chen, Z.Y. Magnetically separable Fe_3O_4/TiO_2 hollow spheres: Fabrication and photocatalytic activity. *J. Phys. Chem. C* **2008**, *113*, 553–558.
14. Stjerndahl, M.; Andersson, M.; Hall, H.E.; Pajerowski, D.M.; Meisel, M.W.; Duran, R.S. Superparamagnetic Fe_3O_4/SiO_2 nanocomposites: Enabling the tuning of both the iron oxide load and the size of the nanoparticles. *Langmuir* **2008**, *24*, 3532–3536.

15. Wang, P.; Shi, Q.H.; Shi, Y.F.; Clark, K.K.; Stucky, G.D.; Keller, A.A. Magnetic permanently confined micelle arrays for treating hydrophobic organic compound contamination. *J. Am. Chem. Soc.* **2008**, *131*, 182–188.

16. Xu, Z.H.; Li, C.X.; Kang, X.J.; Yang, D.M.; Yang, P.P.; Hou, Z.Y.; Lin, J. Synthesis of a multifunctional nanocomposite with magnetic, mesoporous, and near-IR absorption properties. *J. Phys. Chem. C* **2010**, *114*, 16343–16350.

17. Wang, Y.Y.; Li, B.; Zhang, L.M.; Li, P.; Wang, L.L.; Zhang, J. Multifunctional magnetic mesoporous silica nanocomposites with improved sensing performance and effective removal ability toward Hg(II). *Langmuir* **2011**, *28*, 1657–1662.

18. Ma, W.-F.; Zhang, Y.; Li, L.-L.; You, L.-J.; Zhang, P.; Zhang, Y.-T.; Li, J.-M.; Yu, M.; Guo, J.; Lu, H.-J.; Wang, C.-C. Tailor-made magnetic Fe_3O_4@$mTiO_2$ microspheres with a tunable mesoporous anatase shell for highly selective and effective enrichment of phosphopeptides. *ACS Nano* **2012**, *6*, 3179–3188.

19. Ding, H.L.; Zhang, Y.X.; Wang, S.; Xu, J.M.; Xu, S.C.; Li, G.H. Fe_3O_4@SiO_2 core/shell nanoparticles: The silica coating regulations with a single core for different core sizes and shell thicknesses. *Chem. Mater.* **2012**, *24*, 4572–4580.

20. Zhu, G.-T.; Li, X.-S.; Gao, Q.; Zhao, N.-W.; Yuan, B.-F.; Feng, Y.-Q. Pseudomorphic synthesis of monodisperse magnetic mesoporous silica microspheres for selective enrichment of endogenous peptides. *J. Chromatogr. A* **2012**, *1224*, 11–18.

21. Ge, J.P.; Zhang, Q.; Zhang, T.R.; Yin, Y.D. Core-satellite nanocomposite catalysts protected by a porous silica shell: Controllable reactivity, high stability, and magnetic recyclability. *Angew. Chem. Int. Ed.* **2008**, *47*, 8924–8928.

22. Deng, Y.H.; Cai, Y.; Sun, Z.K.; Liu, J.; Liu, C.; Wei, J.; Li, W.; Liu, C.; Wang, Y.; Zhao, D.Y. Multifunctional mesoporous composite microspheres with well-designed nanostructure: A highly integrated catalyst system. *J. Am. Chem. Soc.* **2010**, *132*, 8466–8473.

23. Xuan, S.H.; Wang, F.; Lai, J.M.Y.; Sham, W.Y.; Wang, Y.-X.; Lee, S.-F.; Yu, J.C.; Cheng, C.H.K.; Leung, K.C. Synthesis of biocompatible, mesoporous Fe_3O_4 nano/microspheres with large surface area for magnetic resonance imaging and therapeutic applications. *ACS Appl. Mater. Interfaces* **2011**, *3*, 237–244.

24. Zhu, M.Y; Diao, G.W. Synthesis of porous Fe_3O_4 nanospheres and its application for the catalytic degradation of xylenol orange. *J. Phys. Chem. C* **2011**, *115*, 18923–18934.

25. Liu, H.F.; Ji, S.F.; Zheng, Y.Y.; Li, M.; Yang, H. Modified solvothermal synthesis of magnetic microspheres with multifunctional surfactant cetyltrimethyl ammonium bromide and directly coated mesoporous shell. *Power Technol.* **2013**, *246*, 520–529.

26. Lin, C.; Tao, K.; Hua, D.Y.; Ma, Z.; Zhou, S.H. Size effect of gold nanoparticles in catalytic reduction of *p*-nitrophenol with $NaBH_4$. *Molecules* **2013**, *18*, 12609–12620.

Sample Availability: Samples of the catalyst samples are available from the authors.